Japanese Dental Science Review (2015) 51, 85—95

Available online at www.sciencedirect.com

ScienceDirect

journal homepage: www.elsevier.com/locate/jdsr

Review Article

Synthesis and modification of apatite nanoparticles for use in dental and medical applications

Masahiro Okada, Takuya Matsumoto*

Department of Biomaterials, Graduate School of Medicine, Dentistry and Pharmaceutical Sciences, Okayama University, 2-5-1 Shikata-cho, Kita-ku, Okayama 700-8558, Japan

Received 19 November 2014; received in revised form 26 March 2015; accepted 27 March 2015

KEYWORDS
Hydroxyapatite;
Nanoparticle;
Composite;
Carrier;
Filler

Summary Synthesised hydroxyapatite (HAp) exhibits excellent biocompatibility, making it an ideal candidate for use as a hard tissue substitute material. Nanoscale-size effects and surface phenomena impart HAp nanoparticles with unique properties compared to the conventional-sized HAp ceramics. Modification of HAp is also important for regulating its physiochemical properties. In this review, methods of HAp synthesis and modification, and various applications of HAp nanoparticles for dental and medical treatment are discussed.

Contents

* Corresponding author. Tel.: +81 862356665.
E-mail address: tmatsu@md.okayama-u.ac.jp (T. Matsumoto).

http://dx.doi.org/10.1016/j.jdsr.2015.03.004

1. Introduction

Vertebrate hard tissues consist mainly of inorganic compounds (Table 1 [1]), collectively termed biological apatite. Apatite is a general term for crystalline minerals and can be represented by the formula $M_{10}(ZO_4)_6X_2$. Each component (M, ZO_4, and X) in the formula can be replaced by a large number of different ions listed below [2]:

M = Ca^{2+}, Mg^{2+}, Sr^{2+}, Ba^{2+}, Mn^{2+}, Fe^{2+}, Zn^{2+}, Cd^{2+}, Pb^{2+}, H^+, Na^+, K^+, Al^{3+}, etc.
ZO_4 = PO_4^{3-}, AsO_4^{3-}, VO_4^{3-}, SO_4^{2-}, CO_3^{2-}, SiO_4^{4-}, etc.
X = OH^-, F^-, Cl^-, Br^-, O^{2-}, CO_3^{2-}, vacancy, etc.

The most common apatite found in nature is calcium phosphate apatite, where M and ZO_4 are Ca^{2+} and PO_4^{3-}, respectively. When X is OH^- (*i.e.* $Ca_{10}(PO_4)_6(OH)_2$; stoichiometric Ca/P molar ratio is 1.67), the apatite is named hydroxylapatite [3], traditionally also called as hydroxyapatite (HAp).

Stoichiometric HAp belongs to a hexagonal crystal system [4] and has two major crystal planes: *a* plane and *c* plane (Fig. 1). It is widely believed that the *a* plane is rich in calcium ions and hence positively charged, whereas the *c* plane is rich in phosphate and hydroxide ions and hence negatively charged [7,8]. That is, HAp surfaces exhibit anisotropic characteristics such as anisotropic adsorption profiles for biomolecules [8]. Note that the surface ion composition (and hence, the surface charge) of HAp in aqueous medium varies according to the ion composition of the medium because of ion exchange [9] and gradual dissolution [10].

Synthetic HAp sintered ceramics (in dense, porous, and granular forms) have been used in dental and medical fields [2,11,12], and their applications include alveolar ridge reconstruction and augmentation [13], fillers for bone defects [14], and middle ear implants [15]. HAp is bioactive (osteoconductive); thus, HAp has the ability to encourage bone growth along its surface when placed in the vicinity of viable bone or differentiated bone-forming cells [16]. HAp is one of many types of calcium orthophosphates listed in Table 2 [17], and some other calcium phosphates that show higher solubility than HAp have been also used in dental and medical fields [17,18].

Table 1 Comparative compositions (wt%) of bone, dentine, and enamel [1].

	Bone	Dentine	Enamel
Ca	34.8	35.1	36.5
P	15.2	16.9	17.7
Na	0.9	0.6	0.5
K	0.03	0.05	0.08
CO_2	7.4	5.6	3.5
F	0.03	0.06	0.01
Total inorganics	65	70	97
Total organics	25	20	1.5
Water	10	10	1.5

Biological apatite is a non-stoichiometric form of HAp containing trace ions and deficient Ca^{2+}. The trace ions include positively charged ions (such as Mg^{2+}, Na^+, and K^+) and negatively charged ions (such as CO_3^{2-}, Cl^-, and F^-), and the most common substituting ion is carbonate (CO_3^{2-}), which can replace OH^- and PO_4^{3-}, respectively [4]. Depending on the hard tissue type, biological apatite exhibits different crystal morphologies. For example, in bone tissue, the *c* axes of crystallites (*ca.* 50 nm × 25 nm × 4 nm [19]) are parallel to the extending collagen fibres, resulting in the exposure of the *a* planes on the bone surface. In contrast, in tooth enamel, larger crystallites (*ca.* 100 μm × 25 nm × 70 nm [20]) form enamel prisms extending from the dentino-enamel junction, resulting in *c*-planes that are preferentially parallel to the enamel surface.

Nanoparticles (nanopowders, nanocrystals, or nanostructured particles) are microscopic particles with at least one dimension in the nanometer scale (usually, 100 nm or less). In general, nanoparticles offer improved properties compared with conventional-sized materials because of their large surface-to-volume ratio (specific surface area) [21]. To control the properties of HAp nanoparticles, it is important to control the particle morphology (the exposure of their *a* and *c* planes), which can be achieved by adjusting their synthesis methods. Modification of HAp is also important for the regulation of its physiochemical properties. This paper provides a summary of existing knowledge and recent progress on HAp nanoparticles, from synthesis and modification to dental and medical applications.

2. Synthesis methods for HAp nanoparticles

HAp nanoparticles can be synthesised *via* various methods that are categorised as solid-state and wet-state methods (Table 3).

2.1. Solid-state methods

Solid-state methods are solid-state reactions between raw material powders (*e.g.* $CaHPO_4$ and CaO) induced by thermal treatments, and they usually give stoichiometric and

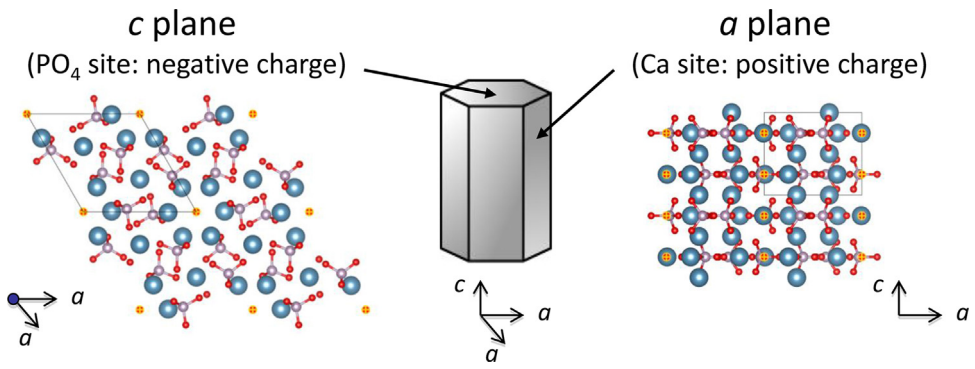

Figure 1 Crystal structure [5] and schematic illustration of stoichiometric hydroxyapatite (HAp). HAp contains both cations and anions in its structure and has high affinity for organic molecules. The blue, white, red and yellow spheres are Ca, P, O, and OH respectively. The crystal structure is drawn with VESTA 3.2.1
Source: Momma and Izumi [6].

well-crystallised HAp, but require relatively high temperatures (mostly exceeding 700 °C) and long treatment times [22,23]. Additionally, HAp synthesised *via* solid-state methods is generally a sintered bulk, and therefore, milling or grinding is necessary to obtain nanoparticles [24]. A mechanochemical method through direct ball milling for the mixture of raw materials can also be used to fabricate HAp nanoparticles in solid state [25,26]. Omori et al. recently developed a Pechini-based method, a type of homogeneous solid-state method, to obtain well-crystallised HAp nanoparticles without milling [27]: a mixture of HAp nanocrystals and CaO matrix was first prepared under non-stoichiometric conditions (Ca/P molar ratio $\gg$ 1.67) at 1000 °C, and then the CaO matrix was removed by washing to obtain well-dispersible HAp nanoparticles.

The plasma technique is another physical method to fabricate nanoparticles in a solid state. Khor et al. used a radiofrequency plasma spray process to fabricate HAp

Table 2 Major calcium phosphates and their properties [16].

Ca/P molar ratio	Chemical formula	Name	Abbr.	Water solubility at 25 °C (g/L)	pH stability range at 25 °C
0.5	$Ca(H_2PO_4)_2{\cdot}H_2O$	Monocalcium phosphate monohydrate	MCPM	~18	0—2
0.5	$Ca(H_2PO_4)_2$	Monocalcium phosphate anhydrous	MCPA	~17	[a]
1.0	$CaHPO_4{\cdot}2H_2O$	Dicalcium phosphate dihydrate (brushite)	DCPD	~0.088	2—6
1.0	$CaHPO_4$	Dicalcium phosphate anhydrous (monetite)	DCPA	~0.0048	[a]
1.2—2.2	$Ca_xH_y(PO_4)_z{\cdot}nH_2O$ (n = 3—4.5)	Amorphous calcium phosphate	ACP	[b]	~5—12[c]
1.33	$Ca_8(HPO_4)_2(PO_4)_4{\cdot}5H_2O$	Octacalcium phosphate	OCP	~0.0081	5.5—7
1.5	α-$Ca_3(PO_4)_2$	α-Tricalcium phosphate	α-TCP	~0.0025	[d]
1.5	β-$Ca_3(PO_4)_2$	β-Tricalcium phosphate	β-TCP	~0.0005	[d]
1.5—1.67	$Ca_{10-x}(HPO_4)_x(PO_4)_{6-x}(OH)_2$ ($0 < x < 1$)	Calcium-deficient hydroxyapatite	CDHA	~0.0094	6.5—9.5
1.67	$Ca_{10}(PO_4)_6(OH)_2$	Hydroxyapatite	HAp	~0.0003	9.5—12
2.0	$Ca_4(PO_4)_2O$	Tetracalcium phosphate (hilgenstockite)	TTCP	~0.0007	[d]

[a] Stable at above 100 °C.
[b] Cannot be measured precisely.
[c] Always metastable.
[d] These compounds cannot be precipitated from aqueous solutions.

Table 3 Synthesis methods for HAp particles.

		Typical particle size[a]	Morphology control	Crystallinity [b]	Ref.
Solid state	Solid-state reaction	—	Impossible	High	[22,23]
	Ball milling	200—500 nm	Poor	High	[24]
	Selective dissolution of binary phase	70—500 nm	Poor	High	[27]
	Calcination with anti-sintering agents	50—300 nm	Easy	High	[29]
	Mechanochemical methods	Micron order	Poor	Poor	[25,26]
	Plasma spraying	100 nm	Poor	Poor	[28]
Wet state	Wet chemical precipitation	50—500 nm	Easy	Poor	[29—32]
	Homogeneous precipitation				
	Thermal pH change	Micron order	Easy	High	[34—38]
	Thermal dissociation of Ca ions	30—500 nm	Easy	High	[39,40]
	Micelle-templated precipitation	30—500 nm	Easy	Poor	[41,42]
	Emulsion method	30—100 nm	Easy	Poor	[43,44]
	Hydrothermal conversion	Micron order	Easy	High	[45—52]
	Hydrothermal crystal growth	30—100 nm	Easy	High	[53—56]
	Sol—gel method	—	Poor	Amorphous	[57—60]

[a] Note that this value does not show the crystal size; rather, it shows the size of particles (including polycrystals or agglomerates) as a dispersed state.
[b] Samples without thermal treatment.

nanoparticles (particle size, 10—100 nm), which contained both amorphous and crystalline phases [28].

2.2. Wet-state methods

Wet-state methods require relatively low temperatures, and nanoparticles can be easily synthesised. However, their crystallinity and Ca/P ratio are lower than those of the well-crystallised stoichiometric HAp synthesised by solid-state methods in many cases; that is, well-crystallised HAp can be obtained only at elevated temperatures *via* post treatments such as hydrothermal treatments and calcination under wet and dry conditions, respectively. Although calcination in the dry state induces the sintering of HAp nanoparticles, a novel calcination method was developed to synthesise well-dispersible HAp nanocrystals [29].

Precipitation methods (wet chemical precipitation) [30,31] have been widely used among the wet-state methods because they are simple. Simple mixing of two aqueous solutions of calcium and orthophosphate (at pH > 7) results in the formation of highly supersaturated solutions of HAp, which induces rapid precipitation of nanoparticles [31] according to the following reactions:

$$10Ca(OH)_2 + 6H_3PO_4 \rightarrow Ca_{10}(PO_4)_6(OH)_2 + 18H_2O \quad (1)$$

$$10Ca(NO_3)_2 + 6(NH_4)_2HPO_4 + 8NH_4OH \rightarrow Ca_{10}(PO_4)_6(OH)_2 + 20NH_4NO_3 + 6H_2O \quad (2)$$

The morphology of HAp nanoparticles depends on the precipitation conditions such as the concentration of reactants, ionic strength, pH, and temperature [21,32] (Fig. 2). The mixing condition of the reactants and the composition of the medium are also important factors. Iijima et al. developed a cation-selective membrane system and found a co-operative role of amelogenin and fluoride in the regulation of crystal orientation and phase, resulting in the formation of fine rod-like apatite whose orientation was similar to that of authentic tooth enamel crystals [33].

Homogeneous precipitation methods start with a homogeneous solution of calcium phosphate (dissolved under acidic conditions), and nucleation and growth of HAp are induced by thermal decomposition of urea (Eq. (3)) [34,35] or acetamide (Eq. (4)) [36]:

$$(NH_2)_2CO + H_2O \rightarrow CO_2 + 2NH_3 \quad (3)$$

$$CH_3CONH_2 + H_2O \rightarrow CH_3COOH + NH_3 \quad (4)$$

The resultant NH_3 increases the solution pH and degree of supersaturation for HAp, leading to the formation (precipitation) of HAp particles. Slow hydrolysis of the molecules at high temperature leads to the formation of large and well-crystallised HAp particles. The hydrolysis of urea is accelerated by the addition of an enzyme (urease), especially at low temperatures [37]. Aizawa et al. recently synthesised plate-shaped HAp particles with preferred exposure of *c* planes by a homogeneous precipitation method using an enzymatic reaction involving urea [38]. The hydrothermal treatment of the homogeneous calcium phosphate solution, in which calcium ions are dissolved by chelation with ethylenediaminetetraacetic acid (EDTA) [39] or citric acid [40], also leads to the formation of HAp particles because of thermal dissociation of calcium chelates in phosphate solutions.

Micelle-templated precipitation methods are conducted in the presence of surfactant micelles as a nanostructured template [41,42]. Micelles form when the concentration of surfactant molecules is higher than the critical micelle concentration (CMC). The shape (sphere, cylinder, or lamellar) and size of a micelle can be controlled by the surfactant molecular geometry and solution conditions (surfactant concentration, temperature, and ionic strength). Yao et al. utilised a micelle-templated method for preparing

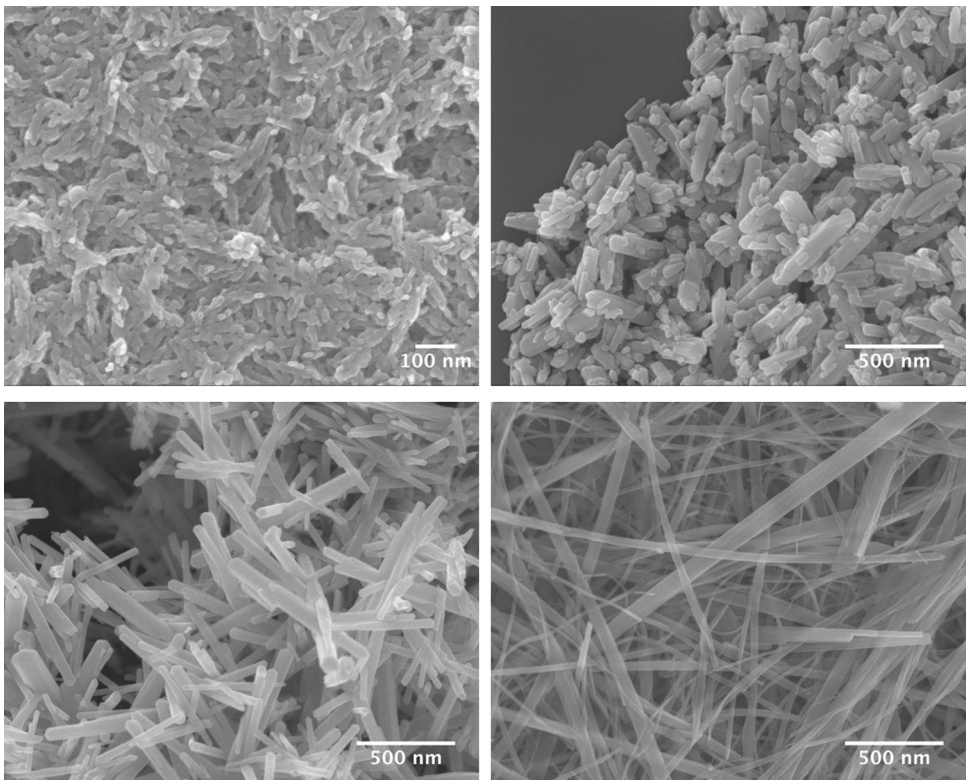

Figure 2 Scanning electron microscopy (SEM) images of HAp nanoparticles with different particle sizes prepared by precipitation methods under different conditions.

mesoporous HAp nanoparticles with 3-nm-sized channels [41]. Ye et al. reported micelle-templated synthesis of HAp hollow nanoparticles or nanotubes (diameter of approximately 35 nm, length of 50—250 nm, and hollow diameter of 13 nm) with polymeric surfactants [42].

Emulsion methods involve precipitation in a restricted space to form small aqueous droplets stabilised in an oil phase with surfactant molecules [43,44]. Morphology control of HAp nanoparticles can be achieved by restricting crystal growth, and this surfactant-based process can inhibit excessive agglomeration of the particles. For example, Lim et al. have prepared HAp nanoparticles by reacting $CaCl_2$ and $(NH_4)_2HPO_4$ in an inverse microemulsion formed with nonionic surfactants in cyclohexane [43], and they found that the microemulsion route led to significant refinement of the particle size and degree of particle agglomeration compared with the particles obtained by a conventional wet chemical precipitation.

The hydrothermal conversion methods involve hydrolysis of calcium phosphates ($CaHPO_4$, $Ca_8(HPO_4)_2(PO_4)_4{\cdot}5H_2O$, $Ca_3(PO_4)_2$, chlorapatite, and fluorapatite) [45—47] or poorly soluble calcium salts ($CaCO_3$ [48,49] and $CaSO_4{\cdot}2H_2O$ [50,51]) into HAp in aqueous medium, generally under high temperature and pressure, by using calcium, phosphate, and/or alkaline sources to control the Ca/P ratio of the products. Microwave irradiation [52] can be used rather than conventional heating in pressure-resistant vessels. Hydrothermal conversion methods generally lead to the formation of large crystalline HAp because of the low number of nucleation sites.

Hydrothermal crystal growth methods are post treatments for low-crystallised HAp nanoparticles (prepared by wet chemical precipitation in many cases) in aqueous medium. The dimensions of the precipitated HAp nanoparticles increase by Ostwald ripening (maturation) under boiling or ambient ageing in aqueous media [53,54]. Pathi et al. recently reported a two-step hydrothermal method to obtain HAp nanoparticles with varying crystallinity and average length (32—103 nm) [55]. Some recent attempts at preparing nanostructured HAp hollow particles without templates did meet with some success. For example, Nathanael et al. reported template-free formation of HAp nanorings with an inner diameter of 70 nm by a combined high-gravity and hydrothermal crystal growth approach [56].

Sol—gel methods have been used for fabricating fine ceramics in liquid medium, typically with metal alkoxide precursors that undergo hydrolysis and polycondensation reactions to form a solid phase [57]. The sol—gel method with calcium alkoxides and/or phosphorus alkoxides is also an effective way to fabricate nanostructured HAp sintered ceramics [58,59]. The obtained solid phase generally consists of amorphous Ca—P intermediates (and/or the mixture of unreacted precursors), and hence, a thermal treatment (generally at 400—500 °C, which is lower than the sintering temperature of HAp powder, approximately 800—1000 °C) is necessary to obtain well-crystallised HAp. The products of sol—gel methods are, therefore, obtained in a sintered polycrystalline form, and hence, grinding or milling is usually necessary to obtain HAp in the nanoparticle form. Recently, Costa et al. prepared microspheres consisting of nanosized

HAp wires (25—800-nm thick) by a combination of sol—gel and hydrothermal (conversion) processes [60].

3. Modification of HAp nanoparticles

3.1. Ion substitution

Modification of HAp has shown remarkable flexibility for regulation of its properties. Ion substitution with cations (such as Mg^{2+}, Sr^{2+}, Zn^{2+}, Fe^{3+}, and Ag^{+}) and/or anions (such as CO_3^{2-}, SiO_4^{3-}, and F^{-}) is one of the ways to alter its biocompatibility, sinterability, and mechanical properties [61,62]. For example, conventional HAp sintered ceramics are hardly resorbed after implantation [63], which is quite different from natural bone minerals, whereas CO_3-substituted apatite nanoparticles exhibit physicochemical characteristics similar to those of bone minerals [64]. Sr substitution has been also found to increase the solubility of apatite [65]. Sr is found in the mineral phase of bone, especially in new bones [66], and Sr substitution has a positive effect on osteoblasts for enhancing alkaline phosphatase (ALP) activity, collagen type I production, and osteocalcin levels [67]. Recent results demonstrated the regulation of zinc (Zn)-substituted apatite and increased performance in terms of protein adsorptive capacity [68] and increased proliferation rate of osteoblast cells *in vitro* [69]. However, biocompatibility is affected by the concentration of metals; the threshold concentration of Zn is reported to be 1.2 wt%, above which Zn ions cause cell toxicity [69].

3.2. Modification with organic molecules

Modification with organic molecules is an alternative way to alter the surface properties of HAp. Surfactant molecules [70], alcohol [71], carboxylic acids [72], poly(ethylene imine) [73], phosphonate-modified poly(ethylene oxide) [74], poly(vinyl alcohol) [75], and biopolymers [76] can be adsorbed on HAp surfaces, and thus, HAp surfaces can be modified by additives. The addition of these molecules during wet-state synthesis (*in situ* modification) also induces morphological changes in HAp nanoparticles through inhibition of crystal growth by preferential adsorption of the additives onto a HAp surface. *In situ* modification with amino acids is also important for controlling the morphology and surface charge of HAp nanoparticles [77—79]. For example, HAp synthesised in the presence of glycine, serine, aspartic acid, and glutamic acid showed morphological changes and increased solubility compared to HAp synthesised in the absence of amino acids; other amino acids (alanine, valine, proline, threonine, hydroxyproline, methionine, arginine, and histidine) did not affect the crystallinity, morphology, or solubility of HAp [78]. It has also been demonstrated that incorporation of aspartic acid onto the HAp surface enhanced the adsorption of basic proteins because of the additional carboxyl groups of aspartic acid [79]. Wu et al. recently revealed that the chirality of the additives plays an important role in the asymmetric crystal growth of apatite [80] by using the L- or D-forms of glutamic acid or aspartic acid.

The surfaces of HAp nanoparticles can be also modified with the above-mentioned organic molecules after synthesis (post modification). Post modification has the advantaged of separation of morphological control and surface modification; that is, the broadening of the choice of organic molecules. For example, the well-crystallised nanoparticles prepared *via* hydrothermal treatments can be modified with thermally instable molecules (such as biomolecules). In addition, chemical modification of the HAp surface *via* a covalent linkage can be achieved by post modification with silane-coupling agents [81] or isocyanates [82,83].

4. Applications of HAp nanoparticles

4.1. Building block for nanostructured ceramics

HAp nanoparticles were found to exhibit improved sinterability (densification) [84,85]. Nanostructured HAp ceramics are also expected to have better bioactivity than conventional HAp ceramics (consisting of coarser crystals) because of their nanoscale topography [86—88]. For example, Webster et al. showed enhanced osteoclast-like cell adhesion and function on nanophase HAp ceramic surfaces [86,87]. Sun et al. reported that nanophase HAp promotes the proliferation and osteogenic differentiation of periodontal ligament cells compared to dense HAp [88]. Recently, nanoparticle-assembled HAp plates with nanosized pores inside the plate were prepared by simply drying an aqueous dispersion of HAp nanoparticles on a liquid substrate at 60 °C without binder molecules (Fig. 3) [89,90]. Feng et al. developed a novel two-step sintering process (selective laser

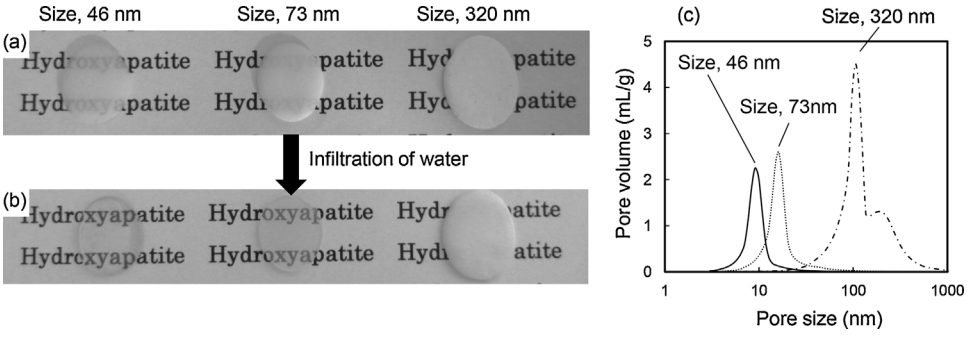

Figure 3 HAp nanoparticle-assembled blocks prepared with nanoparticles with different particle sizes: (a) dry state; (b) wet state; (c) pore size distribution.

sintering (SLS) followed by isothermal sintering at a lower temperature) for fabricating nanostructured HAp scaffolds with high mechanical strength and an interconnected macroporous structure [91].

4.2. HAp nanocomposites

HAp/polymer composites have been developed to overcome the inferior mechanical properties (brittleness and low stiffness) of traditional HAp sintered ceramics (or to improve bioactivity of the polymer matrix) [92]. The original concept of the bioceramics/polymer composite was introduced by Bonfield et al. [93], based on the concept that bone tissue comprises an organic matrix reinforced with a mineral component. The bone analogue HAp/polyethylene composite combines the bioactivity of HAp with the toughness of polyethylene. Further combination with other organic materials such as poly(lactide-co-glycolide) (PLGA) [94,95], collagen [96,97], fibrin [98], and polysaccharide [99] provides optimal mechanical properties and the ability to control cell functions [100]. Recently, click chemistry has been utilised in the design of new biodegradable polymers with improved mechanical strength and with easily clickable surfaces for biofunctionalisation [101]. Sun et al. developed a composite of HAp and clickable biodegradable polymers as a novel class of orthopaedic biomaterial that offers distinct advantages for bone tissue engineering applications [102].

Powder metallurgy processing of HAp nanocrystals with other inorganic materials such as metals (especially titanium (Ti) [103]) or metal oxides (ZrO_2 [104,105], TiO_2 [106], and Al_2O_3 [107]) has also been developed to improve the mechanical characteristics of HAp ceramics or to the improve biocompatibility of metals or metal oxides.

The overall structural design of the composite from the nanoscale to the macroscale level is important for controlling its mechanical and physiochemical properties. HAp composites are generally fabricated by mixing HAp particles with a matrix. However, the bioactivity of HAp can be hindered because most of the HAps are buried inside the composite matrix by simple mixing methods. To coat well-crystallised HAp on a broad range of substrates, the nanocrystal coating method has been developed [108,109]. The HAp nanocrystal coating has been applied to percutaneous devices [110] and injectable cell scaffolds [111]. Freeze casting processing and additive manufacturing have been used for fabricating nanocomposite structures inspired by natural materials (such as nacre or the stomatopod club) to improve the stiffness, strength, and toughness of the structure [112].

4.3. Carriers for drug, protein, and gene delivery

HAp nanoparticles have been investigated as a carrier for growth factors [113,114], antibiotics [115,116], and anticancer drugs [117,118]. The adsorption/desorption characteristics [114,119,120] and conformational changes [121—123] of various types of proteins (or peptides) on HAp surfaces have been studied. Computational (*in silico*) studies have been used to clarify the interaction between proteins (or peptides) and HAp surfaces [124—126].

Calcium phosphate (CaP)-deoxyribonucleic acid (DNA) co-precipitation has been used for *in vitro* gene transfection because of the biocompatible, biodegradable, and easy-to-handle nature of CaP [127]. To achieve effective gene transfection, HAp nanoparticles can be also utilised as gene carriers because of their good ability to absorb DNA molecules [128,129].

4.4. Reparative materials for damaged enamel

The application of HAp to repair damaged enamel has recently attracted attention in the dental field because of the chemical and structural similarity of HAp to tooth minerals [130,131]. Li et al. showed that remineralisation increased by using 20-nm HAp over several hundred nanometer-sized HAp or 20-nm amorphous calcium phosphate (ACP) [132]. Recent research by Huang et al. has demonstrated that HAp nanoparticles have a remineralisation effect on an initial caries lesion, similar to that of fluoride [133]. Kim et al. examined the effect of carbonate apatite nanoparticles to prevent re-staining and alterations of the enamel surface after dental bleaching [134].

5. Summary and future perspectives

Synthetic HAp is a beneficial material for dental and medical applications. The use of HAp nanoparticles has many advantages over conventional-sized HAp bulk ceramics based on the large surface-to-volume ratio, reactivity, and biomimetic morphology of the HAp nanoparticles for applications such as fillers for composites, carriers for drugs, and reparative materials for damaged enamel. Numerous methods have evolved in the past few decades to fabricate more effective HAp nanoparticles and composites. Improvement in the dispersion of HAp nanoparticles in liquid medium (or solid matrices) is important for the application of HAp in the nanoparticle form and as HAp-filled composites [135]. Although the dispersion ability has been improved by adding surfactant molecules, it is necessary to develop another approach because of the toxicity of the surfactant molecules. Recent progress in computational analyses for conformational changes of proteins interacting with HAp surfaces that alter the structure and function of a distant active site will work as a guide for designing nanostructured HAp surfaces to transcend the chemistry of natural minerals. Although nanostructured biomaterials have many potential advantages, it is important to remember that the influence of nanoparticles on human health is not well understood, regardless of whether exposure occurs through the manufacture or implantation of nanomaterials. Thus, further understanding the biological influence of nanosized HAp is essential for the development of their future applications.

Conflict of interest statement

The authors declare no conflict of interest associated with this review.

Acknowledgements

This work was supported in part by Japan Society for the Promotion of Science KAKENHI Grant Numbers 25220912, 25293402 and 26106718 (M.T.).

References

[1] Brown PW, Constantz B. Hydroxyapatite and related materials. Boca Raton: CRC Press; 1994.
[2] Aoki H. Medical applications of hydroxyapatite. Tokyo: Ishiyaku, EuroAmerica Inc.; 1994.
[3] Pasero M, Kampf AR, Ferraris C, Pekov IV, Rakovan J, White TJ. Nomenclature of the apatite supergroup minerals. Eur J Miner 2010;22:163—79.
[4] Elliott JC. Structure and chemistry of the apatites and other calcium orthophosphates. Amsterdam: Elsevier; 1994.
[5] Hughes JM, Cameron M, Crowley KD. Structural variations in natural F, OH and Cl apatites. Am Miner 1989;74: 870—6.
[6] Momma K, Izumi F. VESTA 3 for three-dimensional visualization of crystal, volumetric and morphology data. J Appl Crystallogr 2011;44:1272—6.
[7] Aoki H. Surface design and functions of hydroxyapatite. Surf Sci 1989;10:96—101.
[8] Kawasaki T. Hydroxyapatite as a liquid chromatographic packing. J Chromatogr A 1991;544:147—84.
[9] Somasundaran P, Wang YHC. Surface chemical characteristics and adsorption properties of apatite. In: Misra DN, editor. Adsorption on and surface chemistry of hydroxyapatite. New York: Plenum; 1984. p. 129—49.
[10] Suzuki T, Yamamoto T, Toriyama M, Nishizawa K, Yokogawa Y, Mucalo MR, et al. Surface instability of calcium phosphate ceramics in tissue culture medium and the effect on adhesion and growth of anchorage-dependent animal cells. J Biomed Mater Res 1997;34:507—17.
[11] Jarcho M. Calcium phosphate ceramics as hard tissue prosthetics. Clin Orthop Relat Res 1981;157:259—78.
[12] Hing KA, Best SM, Tanner KE, Revell PA, Bonfield W. Histomorphological and biomechanical characterization of calcium phosphates in the osseous environment. Proc Inst Mech Eng H 1998;212:437—51.
[13] Quinn JH, Kent JN. Alveolar ridge maintenance with solid nonporous hydroxylapatite root implants. Oral Surg Oral Med Oral Pathol 1984;58:511—21.
[14] Froum SJ, Kushner L, Scopp IW, Stahl SS. Human clinical and histologic responses to durapatite implants in intraosseous lesions. Case reports. J Periodontol 1982;53:719—25.
[15] van Blitterswijk CA, Hesseling SC, Grote JJ, Koerten HK, de Groot K. The biocompatibility of hydroxyapatite ceramic: a study of retrieved human middle ear implants. J Biomed Mater Res 1990;24:433—53.
[16] Hench LL, Best S. Ceramics, glasses and glass—ceramics. In: Ratner BD, Hoffman AS, Schoen FJ, Lemons JE, editors. Biomaterials science: an introduction to materials in medicine. 2nd ed. Amsterdam: Elsevier Academic Press; 2004. p. 153—69.
[17] Dorozhkin SV. Amorphous calcium (ortho)phosphates. Acta Biomater 2010;6:4457—75.
[18] Suzuki O. Octacalcium phosphate: osteoconductivity and crystal chemistry. Acta Biomater 2010;6:3379—87.
[19] Weiner S, Wagner HD. The material bone: structure-mechanical function relations. Ann Rev Mater Sci 1998;28:271—98.
[20] Daculsi G, Mentanteau J, Kerebel LM, Mitre D. Length and shape of enamel crystals. Calcif Tissue Int 1984;36:550—5.
[21] Okada M, Furuzono T. Hydroxylapatite nanoparticles: fabrication methods and medical applications. Sci Technol Adv Mater 2012;13:064103.
[22] Fowler BO. Infrared studies of apatites. II. Preparation of normal and isotopically substituted calcium, strontium, and barium hydroxyapatites and spectra-structure-composition correlations. Inorg Chem 1974;13:207—14.
[23] Rao RR, Roopa HN, Kannan TS. Solid state synthesis and thermal stability of HAP and HAP — beta-TCP composite ceramic powders. J Mater Sci Mater Med 1997;8:511—8.
[24] Trakhtenberg IS, Rubshtein AP, Volkova EG, Petrova SA, Fishman AY, Zakharov RG, et al. Effect of mechanical activation on the morphology and structure of hydroxyapatite. Inorg Mater 2011;47:45—50.
[25] Otsuka M, Matsuda Y, Hsu J, Fox JL, Higuchi WI. Mechanochemical synthesis of bioactive material: effect of environmental conditions on the phase transformation of calcium phosphates during grinding. Biomed Mater Eng 1994;4:357—62.
[26] El Briak-BenAbdeslam H, Mochales C, Ginebra MP, Nurit J, Planell JA, Boudeville P. Dry mechanochemical synthesis of hydroxyapatites from dicalcium phosphate dihydrate and calcium oxide: a kinetic study. J Biomed Mater Res A 2003;67:927—37.
[27] Omori Y, Okada M, Takeda S, Matsumoto N. Fabrication of dispersible calcium phosphate nanocrystals via a modified Pechini method under non-stoichiometric conditions. Mater Sci Eng C 2014;42:562—8.
[28] Xu JL, Khor KA, Dong ZL, Gu YW, Kumar R, Cheang P. Preparation and characterization of nano-sized hydroxyapatite powders produced in a radio frequency (RF) thermal plasma. Mater Sci Eng A 2004;374:101—8.
[29] Okada M, Omori Y, Awata M, Shirai T, Matsumoto N, Takeda S, et al. Influence of calcination conditions on dispersibility and phase composition of hydroxyapatite crystals calcined with anti-sintering agents. J Nanoparticle Res 2014;16:2469.
[30] Dorozhkin SV. Nanosized and nanocrystalline calcium orthophosphates. Acta Biomater 2010;6:715—34.
[31] Ferraz MP, Monteiro FJ, Manuel CM. Hydroxyapatite nanoparticles: a review of preparation methodologies. J Appl Biomater Biomech 2004;2:74—80.
[32] Lee WH, Zavgorodniy AV, Loo CY, Rohanizadeh R. Synthesis and characterization of hydroxyapatite with different crystallinity: effects on protein adsorption and release. J Biomed Mater Res A 2012;100:1539—49.
[33] Iijima M, Moradian-Oldak J. Control of apatite crystal growth in a fluoride containing amelogenin-rich matrix. Biomaterials 2005;26:1595—603.
[34] Kinoshita M, Kishioka A, Hayashi H, Itatani K. Preparation of fibrous calcium phosphates by homogenous precipitation method and their thermal changes. Gypsum Lime 1989;219:79—87.
[35] Aizawa M, Ueno H, Itatani K, Okada I. Syntheses of calcium-deficient apatite fibres by a homogeneous precipitation method and their characterizations. J Eur Ceram Soc 2006;26:501—7.
[36] Yasukawa A, Takase H, Kandori K, Ishikawa T. Preparation of calcium hydroxyapatitie using amides. Polyhedron 1994;13:3071—8.
[37] Bayraktar D, Tas AC. Biomimetic preparation of HA powders at 37 °C in urea- and enzyme urease- containing synthetic body fluids. Turk J Med Sci 2000;30:235—45.
[38] Aizawa M, Matsuura T, Zhuang Z. Syntheses of single-crystal apatite particles with preferred orientation to the *a*- and *c*-axes as models of hard tissue and their applications. Biol Pharm Bull 2013;36:1654—61.
[39] Fujishiro Y, Fujimoto A, Sato T, Okuwaki A. Coating of hydroxyapatite on titanium plates using thermal dissociation

of calcium—EDTA chelate complex in phosphate solutions under hydrothermal conditions. J Colloid Interface Sci 1995;173:119—27.
[40] López-Macipe A, Gómez-Morales J, Rodríguez-Clemente R. Nanosized hydroxyapatite precipitation from homogeneous calcium/citrate/phosphate solutions using microwave and conventional heating. Adv Matter 1998;10:49—53.
[41] Yao J, Tjandra W, Chen YZ, Tam KC, Ma J, Soh B. Hydroxyapatite nanostructure material derived using cationic surfactant as a template. J Mater Chem 2003;13:3053—7.
[42] Ye F, Guo H, Zhang H, He X. Polymeric micelle-templated synthesis of hydroxyapatite hollow nanoparticles for a drug delivery system. Acta Biomater 2010;6:2212—8.
[43] Lim GK, Wang J, Ng SC, Gan LM. Processing of fine hydroxyapatite powders via an inverse microemulsion route. Mater Lett 1996;28:431—6.
[44] Furuzono T, Walsh D, Sato K, Sonoda K, Tanaka J. Effect of reaction temperature on the morphology and size of hydroxyapatite nanoparticles in an emulsion system. J Mater Sci Lett 2001;20:111—4.
[45] Ishikawa K, Eanes ED. The hydrolysis of anhydrous dicalcium phosphate into hydroxyapatite. J Dent Res 1993;72:474—80.
[46] Onuma K. Recent research on pseudobiological hydroxyapatite crystal growth and phase transition mechanisms. Prog Cryst Growth Charact Mater 2006;52:223—45.
[47] Suzuki O, Kamakura S, Katagiri T, Nakamura M, Zhao B, Honda Y, et al. Bone formation enhanced by implanted octacalcium phosphate involving conversion into Ca-deficient hydroxyapatite. Biomaterials 2006;27:2671—81.
[48] Jinawath S, Polchai D, Yoshimura M. Low-temperature, hydrothermal transformation of aragonite to hydroxyapatite. Mater Sci Eng C 2002;22:35—9.
[49] Sunouchi K, Tsuru K, Maruta M, Kawachi G, Matsuya S, Terada Y, et al. Fabrication of solid and hollow carbonate apatite microspheres as bone substitutes using calcite microspheres as a precursor. Dent Mater J 2012;31:549—57.
[50] Furuta S, Katsuki H, Komarneni S. Porous hydroxyapatite monoliths from gypsum waste. J Mater Chem 1998;8:2803—6.
[51] Ishikawa K. Bone substitute fabrication based on dissolution-precipitation reactions. Materials 2010;3:1138—55.
[52] Katsuki H, Furuta S, Komarneni S. Microwave- versus conventional-hydrothermal synthesis of hydroxyapatite crystals from gypsum. J Am Ceram Soc 1999;82:2257—9.
[53] Pang YX, Bao X. Influence of temperature, ripening time and calcination on the morphology and crystallinity of hydroxyapatite nanoparticles. J Eur Ceram Soc 2003;23:1697—704.
[54] Loo SCJ, Siew YE, Ho S, Boey FYC, Ma J. Synthesis and hydrothermal treatment of nanostructured hydroxyapatite of controllable sizes. J Mater Sci Mater Med 2008;19:1389—97.
[55] Pathi SP, Lin DD, Dorvee JR, Estroff LA, Fischbach C. Hydroxyapatite nanoparticle-containing scaffolds for the study of breast cancer bone metastasis. Biomaterials 2011;32:5112—22.
[56] Nathanael AJ, Hong SI, Mangalaraj D, Ponpandian N, Chen PC. Template-free growth of novel hydroxyapatite nanorings: formation mechanism and their enhanced functional properties. Cryst Growth Des 2012;12:3565—74.
[57] Hench LL, West JK. The sol—gel process. Chem Rev 1990;90:33—72.
[58] Masuda Y, Matubara K, Sakka S. Synthesis of hydroxyapatite from metal alkoxides through sol—gel technique. J Ceram Soc Japan 1990;98:1266—77.
[59] Layrolle P, Ito A, Takishi T. Sol—gel synthesis of amorphous calcium phosphate and sintering into microporous hydroxyapatite bioceramics. J Am Ceram Soc 1998;81:1421—8.
[60] Costa DO, Dixon SJ, Rizkalla AS. One- and three-dimensional growth of hydroxyapatite nanowires during sol—gel—hydrothermal synthesis. ACS Appl Mater Interfaces 2012;4:1490—9.
[61] Shepherd JH, Shepherd DV, Best SM. Substituted hydroxyapatites for bone repair. J Mater Sci Mater Med 2012;23:2335—47.
[62] Evis Z, Webster T. Nanosize hydroxyapatite: doping with various ions. Adv Appl Ceram 2011;110:311—21.
[63] Klein CP, Driessen AA, de Groot K, van den Hooff A. Biodegradation behavior of various calcium phosphate materials in bone tissue. J Biomed Mater Res 1983;17:769—84.
[64] Cazalbou S, Combes C, Eichert D, Rey C, Glimcher MJ. Poorly crystalline apatites: evolution and maturation in vitro and in vivo. J Bone Miner Metab 2004;22:310—7.
[65] Christoffersen J, Christoffersen MR, Kolthoff N, Barenholdt O. Effects of strontium ions on growth and dissolution of hydroxyapatite and on bone mineral detection. Bone 1997;20:47.
[66] Marie PJ, Ammann P, Boivin G, Rey C. Mechanisms of action and therapeutic potential of strontium in bone. Calcif Tissue Int 2001;69:121.
[67] Capuccini C, Torricelli P, Boanini E, Gazzano M, Giardino R, Bigi A. Interaction of Sr-doped hydroxyapatite nanocrystals with osteoclast and osteoblast-like cells. J Biomed Mater Res A 2009;89:594—600.
[68] Fujii E, Ohkubo M, Tsuru K, Hayakawa S, Osaka A, Kawabata K, et al. Selective protein adsorption property and characterization of nano-crystalline zinc-containing hydroxyapatite. Acta Biomater 2006;2:69—74.
[69] Ito A, Ojima K, Naito H, Ichinose N, Tateishi T. Preparation, solubility, and cytocompatibility of zinc-releasing calcium phosphate ceramics. J Biomed Mater Res 2000;50:178—83.
[70] Yan L, Li Y, Deng ZX, Zhuang J, Sun X. Surfactant-assisted hydrothermal synthesis of hydroxyapatite nanorods. Int J Inorg Mater 2001;3:633.
[71] Nagata F, Yokogawa Y, Toriyama M, Kawamoto Y, Suzuki T, Nishizawa K. Hydrothermal synthesis of hydroxyapatite crystals in the presence of methanol. J Ceram Soc Japan 1995;103:70—3.
[72] Toyama T, Oshima A, Yasue T. Hydrothermal synthesis of hydroxyapatite whisker from amorphous calcium phosphate and the effect of carboxylic acid. J Ceram Soc Japan 2001;109:232.
[73] Shkilnyy A, Friedrich A, Tiersch B, Schöne S, Fechner M, Koetz J, et al. Poly(ethylene imine)-controlled calcium phosphate mineralization. Langmuir 2008;24:2102—9.
[74] Adzamli K, Dorshow RB, Hynes MR, Li D, Nosco DL, Adams MD. Preliminary evaluation of a polyethyleneglycol-stabilized manganese-substituted hydroxylapatite as an intravascular contrast agent for MR angiography. J Magn Reson Imaging 1997;7:204.
[75] Mollazadeh S, Javadpour J, Khavandi A. In situ synthesis and characterization of nano-size hydroxyapatite in poly(vinyl alcohol) matrix. Ceram Int 2007;33:1579—83.
[76] Sinha A, Nayar S, Agrawak AC. Synthesis of nanosized and microporous precipitated hydroxyapatite in synthetic polymers and biopolymers. J Am Ceram Soc 2003;86:357—9.
[77] Matsumoto T, Okazaki M, Nakahira A, Sasaki J, Egusa H, Sohmura T. Modification of apatite materials for bone tissue engineering and drug delivery carriers. Curr Med Chem 2007;14:2726—33.
[78] Matsumoto T, Okazaki M, Inoue M, Hamada Y, Taira M, Takahashi J. Crystallinity and solubility characteristics of hydroxyapatite adsorbed amino acid. Biomaterials 2002;23:2241—7.

[79] Uddin MH, Matsumoto T, Ishihara S, Nakahira A, Okazaki M, Sohmura T. Apatite containing aspartic acid for selective protein loading. J Dent Res 2010;89:488—92.
[80] Wu Y-J, Tsai TWT, Chan JCC. Asymmetric crystal morphology of apatite induced by the chirality of dicarboxylate additives. Cryst Growth Des 2012;12:547—9.
[81] Weetall HH. Storage stability of water-insoluble enzymes covalently coupled to organic and inorganic carriers. Biochem Biophys Acta 1970;212:1—7.
[82] Liu Q, de Wijn JR, van Blitterswijk CA. A study on the grafting reaction of isocyanates with hydroxyapatite particles. J Biomed Mater Res 1998;40:358—64.
[83] Liu Q, de Wijn JR, van Blitterswijk CA. Covalent bonding of PMMA, PBMA, and poly(HEMA)to hydroxyapatite particles. J Biomed Mater Res 1998;40:257—63.
[84] Kothapalli CR, Wei M, Legeros RZ, Shaw MT. Influence of temperature and aging time on HA synthesized by the hydrothermal method. J Mater Sci Mater Med 2005;16:441—6.
[85] Wang J, Shaw LL. Morphology-enhanced low-temperature sintering of nanocrystalline hydroxyapatite. Adv Mater 2007;19:2364—9.
[86] Webster TJ, Ergun C, Doremus RH, Siegel RW, Bizios R. Enhanced osteoclast-like cell functions on nanophase ceramics. Biomaterials 2001;22:1327—33.
[87] Balasundaram G, Sato M, Webster TJ. Using hydroxyapatite nanoparticles and decreased crystallinity to promote osteoblast adhesion similar to functionalizing with RGD. Biomaterials 2006;27:2798—805.
[88] Sun W, Chu C, Wang J, Zhao H. Comparison of periodontal ligament cells responses to dense and nanophase hydroxyapatite. J Mater Sci Mater Med 2007;18:677—83.
[89] Okada M, Furuzono T. Low-temperature synthesis of nanoparticle-assembled, transparent, and low-crystallized hydroxyapatite blocks. J Colloid Interface Sci 2011;360:457—62.
[90] Uehira M, Okada M, Takeda S, Matsumoto N. Preparation and characterization of low-crystallized hydroxyapatite nanoporous plates and granules. Appl Surf Sci 2013;287:195—202.
[91] Feng P, Niu M, Gao C, Peng S, Shuai C. A novel two-step sintering for nano-hydroxyapatite scaffolds for bone tissue engineering. Sci Rep 2014;4:5599.
[92] Dorozhkin SV. Calcium orthophosphate-based biocomposites and hybrid biomaterials. J Mater Sci 2009;44:2343—87.
[93] Bonfield W, Grynpas MD, Tully AE, Bowman J, Abram J. Hydroxyapatite reinforced polyethylene — a mechanically compatible implant material for bone replacement. Biomaterials 1981;2:185—6.
[94] Hong Z, Zhang P, Liu A, Chen L, Chen X, Jing X. Composites of poly(lactide-co-glycolide) and the surface modified carbonated hydroxyapatite nanoparticles. J Biomed Mater Res A 2007;81:515—22.
[95] Petricca SE, Marra KG, Kumta PN. Chemical synthesis of poly(lactic-co-glycolic acid)/hydroxyapatite composites for orthopaedic applications. Acta Biomater 2006;2:277—86.
[96] Schneiders W, Reinstorf A, Pompe W, Grass R, Biewener A, Holch M, et al. Effect of modification of hydroxyapatite/collagen composites with sodium citrate, phosphoserine, phosphoserine/RGD-peptide and calcium carbonate on bone remodelling. Bone 2007;40:1048—59.
[97] Kikuchi M. Hydroxyapatite/collagen bone-like nanocomposite. Biol Pharm Bull 2013;36:1666—9.
[98] Sato T, Kawamura M, Sato K, Iwata H, Miura T. Bone morphogenesis of rabbit bone morphogenetic protein-bound hydroxyapatite—fibrin composite. Clin Orthop Relat Res 1991;263:254—62.
[99] Murugan R, Ramakrishna S. Bioresorbable composite bone paste using polysaccharide based nano hydroxyapatite. Biomaterials 2004;25:3829—35.
[100] Pashuck ET, Stevens MM. Designing regenerative biomaterial therapies for the clinic. Sci Transl Med 2012;4:160sr4.
[101] Guo J, Xie Z, Tran RT, Xie D, Jin D, Bai X, et al. Click chemistry plays a dual role in biodegradable polymer design. Adv Mater 2014;26:1906—11.
[102] Sun D, Chen Y, Tran RT, Xu S, Xie D, Jia C, et al. Citric acid-based hydroxyapatite composite scaffolds enhance calvarial regeneration. Sci Rep 2014;4:6912.
[103] Chenglin C, Jingchuan Z, Zhongda Y, Shidong W. Hydroxyapatite-Ti functionally graded biomaterial fabricated by powder metallurgy. Mater Sci Eng A 1999;271:95—100.
[104] Matsumoto TJ, An SH, Ishimoto T, Nakano T, Matsumoto T, Imazato S. Zirconia—hydroxyapatite composite material with micro porous structure. Dent Mater 2011;27:e205—12.
[105] An SH, Matsumoto T, Miyajima H, Nakahira A, Kim KH, Imazato S. Porous zirconia/hydroxyapatite scaffolds for bone reconstruction. Dent Mater 2012;28:1221—31.
[106] Que W, Khor KA, Xu JL, Yu LG. Hydroxyapatite/titania nanocomposites derived by combining high-energy ball milling with spark plasma sintering processes. J Eur Ceram Soc 2008;28:3083—90.
[107] Kim S, Kong YM, Lee IS, Kim HE. Effect of calcinations of starting powder on mechanical properties of hydroxyapatite—alumina bioceramic composite. J Mater Sci Mater Med 2002;13:307—10.
[108] Furuzono T, Kishida A, Tanaka J. Nano-scaled hydroxyapatite/polymer composite. I. Coating of sintered hydroxyapatite particles on poly(gamma-methacryloxypropyl trimethoxysilane)grafted silk fibroin fibers through chemical bonding. J Mater Sci Mater Med 2004;15:19—23.
[109] Okada M, Furukawa K, Serizawa T, Yanagisawa Y, Tanaka H, Kawai T, et al. Interfacial interactions between calcined hydroxyapatite nanocrystals and substrates. Langmuir 2009;25:6300—6.
[110] Furuzono T, Ueki M, Kitamura H, Oka K, Imai E. Histological reaction of sintered nanohydroxyapatite-coated cuff and its fibroblast-like cell hybrid for an indwelling catheter. J Biomed Mater Res B Appl Biomater 2009;89:77—85.
[111] Mima Y, Fukumoto S, Koyama H, Okada M, Tanaka S, Shoji T, et al. Enhancement of cell-based therapeutic angiogenesis using a novel type of injectable scaffolds of hydroxyapatite—polymer nanocomposite microspheres. PLoS ONE 2012;7:e35199.
[112] Wegst UG, Bai H, Saiz E, Tomsia AP, Ritchie RO. Bioinspired structural materials. Nat Mater 2014, http://dx.doi.org/10.1038/nmat4089 [Epub ahead of print].
[113] Gorbunoff MJ, Timasheff SN. The interaction of proteins with hydroxyapatite. III. Mechanism. Anal Biochem 1984;136:440—5.
[114] Matsumoto T, Okazaki M, Inoue M, Yamaguchi S, Kusunose T, Toyonaga T, et al. Hydroxyapatite particles as a controlled release carrier of protein. Biomaterials 2004;25:3807—12.
[115] Kano S, Yamazaki A, Otsuka R, Ohgaki M, Akao M, Aoki H. Application of hydroxyapatite—sol as drug carrier. Biomed Mater Eng 1994;4:283—90.
[116] Uskoković V, Desai TA. Phase composition control of calcium phosphate nanoparticles for tunable drug delivery kinetics and treatment of osteomyelitis. II. Antibacterial and osteoblastic response. J Biomed Mater Res A 2013;101:1427—36.
[117] Barroug A, Glimcher MJ. Hydroxyapatite crystals as a local delivery system for cisplatin: adsorption and release of cisplatin in vitro. J Orthop Res 2002;20:274—80.

[118] Dorozhkin SV, Epple M. Biological and medical significance of calcium phosphates. Angew Chem Int Ed Engl 2002;41:3130—46.
[119] Paul W, Sharma CP. Development of porous spherical hydroxyapatite granules: application towards protein delivery. J Mater Sci Mater Med 1999;10:383—8.
[120] Ikoma T, Tagaya M, Hanagata N, Yoshioka T, Chakarov D, Kasemo B, et al. Protein adsorption on hydroxyapatite nanosensors with different crystal sizes studied in situ by a quartz crystal microbalance with the dissipation method. J Am Ceram Soc 2009;92:1125—8.
[121] Yongli C, Xiufang Z, Yandao G, Nanming Z, Tingying Z, Xinqi S. Conformational changes of fibrinogen adsorption onto hydroxyapatite and titanium oxide nanoparticles. J Colloid Interface Sci 1999;214:38—45.
[122] Capriotti LA, Beebe Jr TP, Schneider JP. Hydroxyapatite surface-induced peptide folding. J Am Chem Soc 2007;129:5281—7.
[123] Goobes G, Goobes R, Schueler-Furman O, Baker D, Stayton PS, Drobny GP. Folding of the C-terminal bacterial binding domain in statherin upon adsorption onto hydroxyapatite crystals. Proc Natl Acad Sci USA 2006;103:16083—8.
[124] Rimola A, Sakhno Y, Bertinetti L, Lelli M, Martra G, Ugliengo P. Toward a surface science model for biology: glycine adsorption on nanohydroxyapatite with well-defined surfaces. J Phys Chem Lett 2011;2:1390—4.
[125] Jimenez-Izal E, Chiatti F, Corno M, Rimola A, Ugliengo P. Glycine adsorption at nonstoichiometric (010) hydroxyapatite surfaces: a B3LYP study. J Phys Chem C 2012;116:14561—7.
[126] Rimola A, Aschi M, Orlando R, Ugliengo P. Does adsorption at hydroxyapatite surfaces induce peptide folding? Insights from large-scale B3LYP calculations. J Am Chem Soc 2012;134(26):10899—910.
[127] Chen C, Okayama H. High-efficiency transformation of mammalian cells by plasmid DNA. Mol Cell Biol 1987;7:2745—52.
[128] Kumta PN, Sfeir C, Lee DH, Olton D, Choi D. Nanostructured calcium phosphates for biomedical applications: novel synthesis and characterization. Acta Biomater 2005;1:65—83.
[129] Kimura T, Nibe Y, Funamoto S, Okada M, Furuzono T, Ono T, et al. Preparation of a nanoscaled poly(vinyl alcohol)/hydroxyapatite/DNA complex using high hydrostatic pressure technology for in vitro and in vivo gene delivery. J Drug Deliv 2011;2011:962743.
[130] Hannig M, Hannig C. Nanomaterials in preventive dentistry. Nat Nanotechnol 2010;5:565—9.
[131] Yamagishi K, Onuma K, Suzuki T, Okada F, Tagami J, Otsuki M, et al. Materials chemistry: a synthetic enamel for rapid tooth repair. Nature 2005;433(February (7028)):819.
[132] Li L, Pan H, Tao J, Xu X, Mao C, Gu X, et al. Repair of enamel by using hydroxyapatite nanoparticles as the building blocks. J Mater Chem 2008;18:4079—84.
[133] Huang SB, Gao SS, Yu HY. Effect of nano-hydroxyapatite concentration on remineralization of initial enamel lesion in vitro. Biomed Mater 2009;4:034104.
[134] Kim YS, Kwon HK, Kim BI. Effect of nano-carbonate apatite to prevent re-stain after dental bleaching in vitro. J Dent 2011;39:636—42.
[135] Šupová M. Problem of hydroxyapatite dispersion in polymer matrices: a review. J Mater Sci Mater Med 2009;20:1201—13.